Symmetry, Stability, Geometric Phases, and Mechanical Integrators (Part I)

J. E. Marsden, O. M. O'Reilly†, F. J. Wicklin‡, B. W. Zombro§*

New analytical techniques and recent algorithms which numerically compute the time evolution of mechanical systems enable today's scientists, engineers, and mathematicians to predict events more accurately and more rapidly than ever before. Beyond the problems of simulation and prediction, however, lie the problems of *understanding* a dynamical system and choosing a correct dynamical system to *model* a given physical situation. Many systems remain too intricate to fully understand, but modern methods of mathematical analysis can sometimes offer insight. Most of this insight is obtained by viewing dynamics geometrically, and in fact the recent advances in mechanics which we review in this article all share this geometric perspective. Much of the value of these techniques lies in their applications, and although applications exist in a broad range of disciplines, we will focus on examples from space mechanics and robotics because these are simple to visualize.

A key problem in space mechanics is the problem of efficiently and effectively controlling the attitude of satellites in their orbits. Several spacecraft, including the very first U.S. satellite, Explorer I, have been unable to complete their missions because they began to tumble in space and could not be stabilized. Much research has been devoted to prevent current orbiting telescopes from suffering a similar fate. These telescopes must be controlled with high precision, since small errors can seriously degrade observations made of objects thousands of light years away. Several problems have plagued the Hubble Space Telescope, including low-frequency vibrations in the structure's solar-power panels due to unanticipated thermal expansion effects as the telescope passes from night into day. These vibrations were further amplified by the telescope's computer controlled stabilization mechanisms (Wilford, [1990]). Two of the topics we shall discuss—stability and numerical integration—are pertinent to the analysis and control of such vibrations.

Stability and control are also important issues in the field of robotics. This is certainly the case for a team at the MIT Artificial Intelligence Laboratory which is trying to construct a somersaulting robot (Hodgins and Raibert [1989]) as shown in Figure 1. Specifically, the project is to build a robot which will gather a running start, launch itself into the air, complete a forward revolution, and then land firmly on its feet. As might be imagined, the challenges involved in such a venture are formidable.

Recent ideas of Berry [1984, 1985], Hannay [1985], and Montgomery [1990], however, may help to solve this problem as well as provide the means for a way of efficiently controlling mechanical systems such as orbiting telescopes. It is amusing to note that many of these recent ideas are related to a natural curiosity that has fascinated and motivated investigations in physiology as well as dynamics: How does a falling cat often manage to land upright even if released while upside down from a complete rest? (See Figure 2.) The cat cannot violate the conservation of angular momentum, yet somehow it manages to turn itself 180 degrees in mid-air. This process has been investigated many times over the past century (see *Nature* [1894], Crabtree [1909], Kane and Scher [1969] and references therein) and recently has been analyzed by Montgomery [1990] with an emphasis on how the cat (or, more generally, a deformable body) can efficiently readjust its orientation by changing its shape. By "efficiently," we mean that the reorientation minimizes some function—for example the total energy expended. Montgomery's results characterize the deformations which allow a cat to most efficiently reorient itself without violating conservation of angular momentum.

We begin with a review of Hamiltonian systems and canonical formulations. We then introduce noncanonical formulations and the concept of reduction of dynamics. Recent results in determining stability are presented in the next section, and these are followed by a discussion of geometric phases in mechanics. We conclude with a survey of some recent advances in numerical integration algorithms.

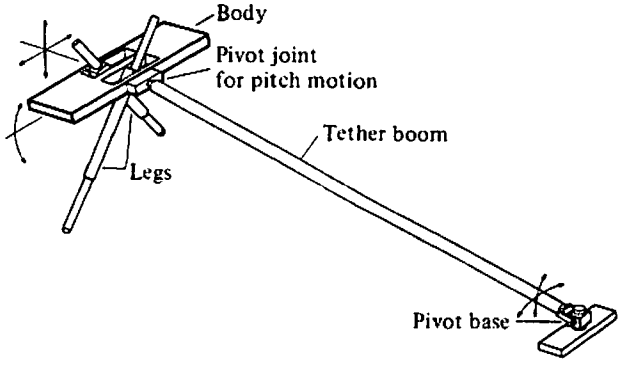

Figure 1: Diagram of the planar biped robot constructed at MIT (from Hodgins and Raibert [1990]). The robot is designed to take a running start, jump into the air, pitch itself forward so that it completes a forward flip, and continue running when it lands. ©1990 MIT Press, used by permission.

Department of Mathematics, University of California, Berkeley, CA 94720.
†Department of Theoretical and Applied Mechanics, Cornell University, Ithaca, NY 14853. Research partially supported by NSF Grant DMS-8703656.
‡Center for Applied Mathematics, Cornell University, Ithaca, NY 14853. Research partially supported by NSF Graduate Fellowship.
§Department of Theoretical and Applied Mechanics, Cornell University, Ithaca, NY 14853.

Figure 2: A falling cat manages to land on its feet even if released upside down without initial angular momentum. The explanation of this counter-intuitive feat may lead to new ways of controlling the dynamics of mechanical systems such as robots and space telescopes (drawing from R. Montgomery *Commun. Math. Phys.* 128, 567 [1990].)

Hamiltonian Formulation

The equations of motion for a classical mechanical system consisting of n particles may be written as a set of first order equations in the form established by Hamilton:

$$\dot{q}^i = \frac{\partial H}{\partial p_i}, \qquad \dot{p}_i = -\frac{\partial H}{\partial q^i}, \quad i = 1, \ldots, n. \quad \text{(CHE)}$$

The generalized configuration coordinates $(q^1, \ldots, q^n)$ and momenta $(p_1, \ldots, p_n)$ together define the system's instantaneous state, which may also be regarded as the coordinates of a point in a $2n$-dimensional vector space called the *phase space*. We denote such a point by $(\mathbf{q},\mathbf{p})$. The *Hamiltonian function* $H(\mathbf{q},\mathbf{p})$ completely defines the system. In the absence of constraining forces and time dependence, $H(\mathbf{q},\mathbf{p})$ is simply the total energy of the system.

In the modern theory of Hamiltonian systems, this classical setting is generalized in two essential ways. First, the phase space, which identifies the possible states of the system, is allowed to be a differentiable manifold rather than merely a linear vector space. This generalization allows for the simplest and most natural characterization of systems consisting of bodies whose motions are spatially constrained. The set of all possible spatial positions of bodies in the system is known as the *configuration space*. For example, the configuration space for a three dimensional rigid body moving freely in space is $SE(3)$, the six dimensional group of Euclidean (rigid) transformations of three-space, that is, all possible rotations and translations. If translations are ignored and only rotations are considered, then the configuration space is $SO(3)$.

When the constraints defining a system are complicated, the configuration space may be an equally complicated manifold. For example, if two rigid bodies are connected at a point by an idealized ball-in-socket joint, then to specify the position of the bodies. we must specify a single translation (since the bodies are coupled) but we need to specify two rotations (since the bodies are free to rotate in any manner). The configuration space is therefore $SE(3) \times SO(3)$. This is already a fairly complicated object, but remember that one must keep track of both positions *and* momenta of each component body in order to formulate the system's dynamics completely. If Q denotes the configuration space (only positions), then the corresponding phase space P (positions and momenta) is the manifold known as the *cotangent bundle* of Q, which is denoted by T^*Q. Describing dynamics on such a manifold in terms of standard vector calculus can be quite cumbersome and computationally costly, but the modern theory of Hamiltonian systems allows us to take advantage of the powerful *differential calculus on manifolds*.

The second important way in which the modern theory of Hamiltonian systems generalizes the classical theory is by relaxing the requirement of using canonical phase space coordinate systems, i.e., coordinate systems for which the equations of motion take the standard form (CHE). An arbitrary transformation of the coordinates $(\mathbf{q},\mathbf{p})$ does not necessarily result in a system in which the new coordinates obey the canonical equations. As a simple example, the canonical description of the simple harmonic oscillator is defined by the Hamiltonian $H(q,p) = (q^2 + p^2)/2$, but if we change variables according to $q = xy$ and $p = y$, then it is easy to verify that x and y are not canonical coordinates.

Canonical coordinates are sometimes convenient variables through which to study Hamiltonian systems, but rigid body dynamics, celestial mechanics, robotics, and biomechanics provide a rich supply of examples of systems for which canonical coordinates are unwieldy and awkward. The free motion of a rigid body in space is the simplest such example. It was treated by Euler in the 18th century and yet it remains remarkably rich as an illustrative example.

As mentioned earlier, the rigid body problem in its primitive formulation has the six dimensional configuration space $SE(3)$. This means that the phase space, $T^*SE(3)$, is twelve dimensional. Assuming that no external forces act on the body, conservation of linear momentum allows us to solve for the components of the position and momentum vectors of the center of mass. This reduces the problem to finding the body's rotational orientation in space as if its center of mass were fixed. Each possible orientation corresponds to an element of the rotation group $SO(3)$, which we may view as a configuration space for all non-trivial motions of the body.

Euler formulated a description of the body's orientation in space in terms of three angles between axes which are either fixed in space or are attached to symmetry planes of the body's motion, as shown in Figure 3. The three *Euler angles*, ψ, ϕ, and θ, are generalized coordinates for the problem.

It is possible to construct a canonical Hamiltonian of the body's rotational motion in terms of the three Euler angles and their conjugate momenta. This leads to a fairly complicated system of six coupled ordinary differential equations. Euler's formulation, however, is simpler than the canonical Hamiltonian approach. Assuming that no external moments act on the body, the angular momentum vector is conserved. Euler used this fact to write the three associated momentum equations in a coordinate system fixed *within the body* rather than fixed in space. Letting (Π_1, Π_2, Π_3) denote the components of the angular momentum vector $\mathbf{\Pi} = \mathbf{\Pi}(t)$ along the principal inertial axes of the body, the momentum equations are given by the well-known *Euler equations:*

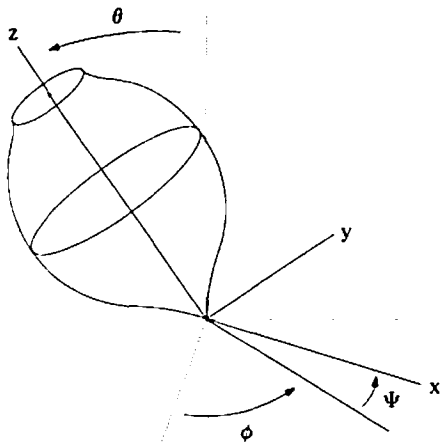

Figure 3: Diagram of Euler angles θ, φ, ψ in the case of a symmetric top. (After Goldstein [1980]).

$$\begin{aligned}\dot{\Pi}_1 &= \frac{I_2 - I_3}{I_2 I_3}\Pi_2\Pi_3,\\ \dot{\Pi}_2 &= \frac{I_3 - I_1}{I_3 I_1}\Pi_3\Pi_1,\\ \dot{\Pi}_3 &= \frac{I_1 - I_2}{I_1 I_2}\Pi_1\Pi_2,\end{aligned} \qquad \text{(EE)}$$

where the constants I_1, I_2 and I_3 are the principal moments of inertia of the body. It was Arnold [1966a] who first clarified in a satisfactory way the relationships between the various representations (body, space, Euler angles) of the equations and showed how the same ideas apply to fluid mechanics as well.

The formulation above is remarkable for the simplicity of its geometrical interpretation. Viewing (Π_1, Π_2, Π_3) as coordinates in a three dimensional vector space, the Euler equations are evolution equations for a point in this space. An integral (constant) of motion for the system is given by the magnitude of the angular momentum vector: $\|\mathbf{\Pi}\|^2 = \Pi_1^2 + \Pi_2^2 + \Pi_3^2$. This can be verified directly from the Euler equations (EE). Because of this, the evolution in time of any initial point $\mathbf{\Pi}(0)$ is constrained to the sphere $\|\mathbf{\Pi}\| = \|\mathbf{\Pi}(0)\| =$ constant. Thus we may view the Euler equations as describing a two dimensional evolution on an invariant sphere. We call this sphere the *reduced* phase space for the rigid body equations. The constant $\|\mathbf{\Pi}\|$ may be interpreted as a parameter which determines the size of the invariant sphere.

A basic fact about this description is that *this two dimensional system is a Hamiltonian system on the two-sphere* S^2. The Hamiltonian structure is not obvious from Euler's equations because the description in terms of angular momentum is inherently non-canonical. This means that there is no way to choose a pair of coordinates from (Π_1, Π_2, Π_3) to satisfy the canonical Hamilton equations (CHE). As mentioned above, however, Hamiltonian systems may be generalized to include Euler's formulation. The Hamiltonian for the reduced system is

$$H = \frac{1}{2}\left(\frac{\Pi_1^2}{I_1} + \frac{\Pi_2^2}{I_2} + \frac{\Pi_3^2}{I_3}\right), \qquad \text{(RBH)}$$

and we shall shortly show how this function allows us to recover Euler's equations (EE). Since solutions curves of (EE) are confined to the level sets of H (which are in general ellipsoids) as well as to the invariant spheres $\|\mathbf{\Pi}\| =$ constant, the intersection of these surfaces are precisely the trajectories of the rigid body, shown in Figure 4.

When considering a reduced phase space such as the sphere in the case of the rigid body equations, we call the fixed points *relative equilibria*. The equilibria are "relative" in the sense that they are equilibria only on the reduced phase space. These equilibria correspond to periodic orbits in the unreduced phase space, specifically to steady rotations about a principal inertial axis. The locations and stability types of the relative equilibria for the rigid body are clear from Figure 4. The four points located at the intersections of the invariant sphere with the x and z axes correspond to pure rotational motions of the body about its major and minor principal axes. These motions are stable, whereas the other two relative equilibria corresponding to rotations about the intermediate principal axis are unstable.

We shall shortly see how the stability analysis for a large class of more complicated systems can be greatly simplified through a careful choice of non-canonical coordinates. We managed to visualize the trajectories of the rigid body without really doing any calculations, but this occurrence is rare; the rigid body is a rather special system. Not only is the rigid body problem completely integrable (one can write down the solution in terms of integrals), but the problem reduces in some sense to a two dimensional manifold and allows questions about trajectories to be phrased in terms of level sets of integrals. Many Hamiltonian systems are not completely integrable and trajectories must be studied numerically. However, the fact that we were able to reduce the number of dimensions in the problem (from twelve to two) and the fact that this reduction was accomplished by appealing to non-canonical coordinates turns out to be a general feature of Hamiltonian systems with symmetry. One of the major results of contemporary theoretical mechanics has been the rigorous formalization of a general reduction procedure.

One of the most attractive features of the reduction procedure is that it may be applied to non-integrable or chaotic systems just as easily as to integrable ones. In a Hamiltonian context, non-integrability is generally taken to mean that, once the "ob-

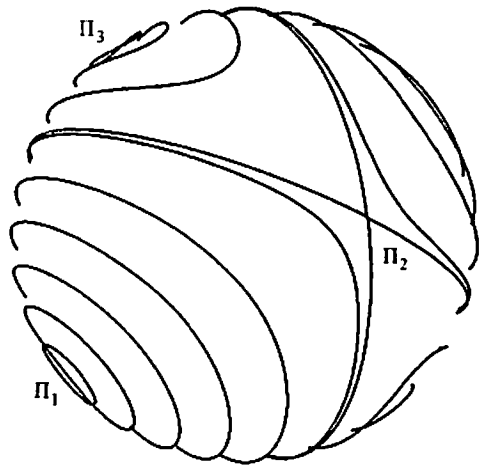

Figure 4: Phase portrait for the rigid body. The magnitude of the angular momentum vector determines a sphere. The intersection of the sphere with the ellipsoids of constant Hamiltonian gives the trajectories of the rigid body. This figure, as well as Figures 12, 13, and 14, were produced using the software package kaos which may be obtained from John Guckenheimer, Cornell University. Figure provided by Mark Meyers.

vious'' integrals are removed any analytic constant of motion is function of the Hamiltonian. We will not attempt to formulate a general definition of chaos, but rather use the term in a loose way to refer to systems whose motion is so extremely complicated that long-term prediction of dynamics is virtually impossible. It can sometimes be very difficult to establish whether a given system is chaotic or non-integrable. Sometimes theoretical tools such as ''Melnikov's method'' (cf. Guckenheimer and Holmes [1983] and Wiggins [1988]) are available. Other times, one resorts to numerics or direct observation. For instance, numerical integration suggests that irregular natural satellites such as Saturn's moon, Hyperion, tumble in their orbits in a highly irregular manner (Wisdom, Peale, and Mignard [1984]). The equations of motion for an irregular body in the presence of a non-uniform gravitational field are similar to the Euler equations except that there is a configuration-dependent gravitational moment term in the equations which may render the system non-integrable.

The evidence that Hyperion tumbles chaotically in space leads to difficulties in numerically modelling this system. It turns out that the manifold $SO(3)$ cannot be covered by a single three dimensional coordinate chart such as the Euler angle chart. Hence, an integration algorithm using canonical variables must employ more than one coordinate system, alternating between coordinates on the basis of the body's current configuration. For a body which tumbles in a complicated fashion, the body's configuration might switch from one chart of $SO(3)$ to another in a very short time interval. In the worst case, this could entail switching coordinate charts at nearly every step of the integration algorithm. The computational cost for such a procedure could be prohibitive. This situation is worse still for odies with internal degrees of freedom like robots and large-cale space structures. Such examples dramatically point out the need to go beyond canonical formulations in the context of practical problems.

Geometry, Symmetry, and Reduction

To motivate the discussion that follows, let us recap the two major elements of our discussion of the problem of the free rigid body: (1) The equations of motion for a system may be simpler in terms of non-canonical coordinates (e.g., Euler's equations) than in canonical coordinates; (2) The essential dynamics of a system may be described in terms of trajectories on a manifold (e.g., the invariant momentum sphere) which has a lower dimension than the dimension of the problem's original phase space. The reduction of dimension involved may be difficult to recognize and cumbersome to formulate within a canonical framework.

We now describe how modern developments in mechanics have led to coordinate-free formulations of equations of motion. These provide a framework for the non-canonical formulation of problems. We then outline a general method for reducing the dimension of the phase space of a Hamiltonian system provided that the system is invariant under an appropriate symmetry group.

We have emphasized the distinction between canonical and non-canonical coordinates by contrasting Hamilton's (canonical) equations with Euler's equations. We may view this distinction from a different perspective by introducing *Poisson bracket* notation. Given two smooth (C^∞) real-valued functions F and H defined on the phase space of a Hamiltonian system, efine the (canonical) Poisson bracket of F and H by

$$\{F,H\} = \sum_{i=1}^{n} \left(\frac{\partial F}{\partial q^i} \frac{\partial H}{\partial p_i} - \frac{\partial H}{\partial q^i} \frac{\partial F}{\partial p_i} \right),$$

where every (q^i,p_i) is a conjugate pair of canonical coordinates. Now suppose that H is the Hamiltonian function for the system. Then the formula for the Poisson bracket is precisely the directional derivative of F along the flow, that is,

$$\dot{F} = \{F,H\}.$$

In particular, Hamilton's equations themselves are recovered if we let F be each of the canonical coordinates in turn:

$$\dot{q}^i = \{q^i,H\} = \frac{\partial H}{\partial p_i}, \qquad \dot{p}_i = \{p_i,H\} = -\frac{\partial H}{\partial q^i}.$$

Once H is specified, the statement ''$\dot{F} = \{F,H\}$ for all smooth functions F'' is equivalent to Hamilton's equations. In fact, it tells how *any* function F evolves along the flow.

This representation of the canonical equations of motion leads to a generalization of the bracket notation to cover non-canonical formulations. There is an appropriate definition of the binary operation $\{\ ,\ \}$ such that the equations of motion in the given coordinates are equivalent to $\dot{F} = \{F,H\}$ which is valid in any system of coordinates. This holds for Hamiltonian systems on reduced phase spaces, such as the angular momentum sphere of the free rigid body, as well as systems expressed in their unreduced forms.

As an example, we once again consider Euler's equations. The solution to the equations are trajectories given in terms of the coordinates (Π_1, Π_2, Π_3) of the three dimensional ''angular momentum space,'' and the constraint $\|\mathbf{\Pi}\|$ = constant reduces the dynamics to a sphere imbedded in this space. We define the following non-canonical bracket of smooth functions on the angular momentum space

$$\{F,H\} = -\mathbf{\Pi} \cdot (\nabla F \times \nabla H),$$

where the gradients are taken with respect to the (Π_1, Π_2, Π_3) coordinates. The geometry of the scalar triple product operation insures that the induced bracket of functions defined on any invariant sphere is represented by the same formula. If H is the rigid body Hamiltonian (see (RBH)) and F is, in turn, allowed to be each of the three coordinate functions Π_i, then the formula $\dot{F} = \{F,H\}$ yields the three Euler equations.

The non-canonical bracket corresponding to the reduced free rigid body problem is an example of what is known as a *Lie-Poisson bracket* (see Appendix A). Other bracket operations have been developed to handle a wide variety of Hamiltonian problems in non-canonical form, including some problems outside of the framework of traditional Newtonian mechanics (see, for instance, Arnold [1966a] or Marsden et al. [1983]). The generalization of the Poisson bracket exemplifies the geometrical emphasis of modern theoretical mechanics. When studying Hamiltonian dynamics from a geometrical perspective, it is essential to distinguish features of the dynamics which depend on the Hamiltonian function from those which depend only on properties of the phase space. The generalized bracket operation is a geometrical invariant in the sense that it depends only on the structure of the phase space. The phase spaces arising in mechanics often have an additional geometrical structure closely related to the Poisson bracket. Specifically, they may be equipped with a certain differential two-form called the *symplectic form*. The symplectic form defines the geometry of a *symplectic manifold* much as the metric tensor defines the geometry of a Riemannian manifold. Bracket operations can be defined entirely in terms of the symplectic form without reference to a particular coordinate system. (See Marsden et al. [1983].)

The classical concept of a *canonical transformation* can also be given a more geometrical definition within this framework.

A canonical transformation is classically defined as a transformation of phase space which takes one canonical coordinate system to another. The modern analogue of this concept is a *symplectic map*—a smooth map of a symplectic manifold to itself which preserves the symplectic form or, equivalently, the Poisson bracket operation. Symplectic maps of cotangent bundles arise naturally in mechanics since every smooth map on a configuration space induces a symplectic map on the cotangent bundle of that space. This induced map is known as a *cotangent lift*.

The geometry of symplectic manifolds is an essential ingredient in the formulation of the reduction procedure for Hamiltonian systems with symmetry. We now outline some important ingredients of this procedure. Some additional information is contained in Appendix A. In Euler's problem of the free rotation of a rigid body in space (assuming that we have already exploited conservation of linear momentum), the six dimensional phase space is $T^*SO(3)$—the cotangent bundle of the three dimensional rotation group. The reduction from six to two dimensions is classically described as a consequence of two essential features of the problem:

(1) the existence of a coordinate system in which the Hamiltonian can be expressed independently of the body's configuration, and

(2) the existence of a conserved quantity, μ, the angular momentum in space.

Condition (1) is equivalent to rotational invariance of the Hamiltonian, while condition (2) expresses the conservation of the total angular momentum of the rigid body. These two conditions are generalized to arbitrary mechanical systems with symmetry in the general reduction theory of Meyer [1973] and Marsden and Weinstein [1974], which was inspired by the seminal works of Arnold [1966a] and Smale [1970]. In this theory, one begins with a given phase space that we denote by P. We assume there is a group G of symmetry transformations of P that transform P to itself by canonical transformations. Generalizing (1) above, one assumes that the Hamiltonian is invariant under these transformations. Generalizing (2), we use the symmetry group to generate a vector-valued conserved quantity which we denote J; it is called the *momentum map*.

Analogous to the set where the total angular momentum has a given value, we consider the set of all phase space points where J has a given value μ. We call this set the μ-level set for J. The analogue of the two dimensional body angular momentum sphere in Figure 4 is the reduced phase space, denoted P_μ, that is constructed as follows: P_μ is the μ-level set for J with any two points that can be transformed one to the other by a group transformation, identified. This identification procedure is not unlike the procedure one uses to bend an interval into a circle by identifying the two endpoints of the interval—what were two points before become one point in the new system. In the reduction theorem, many points can get identified with one new point, but the idea is the same. The reduction process states that P_μ inherits the symplectic (or Poisson bracket) structure from that of P, so it can be used as a new phase space. Also, dynamical trajectories of the Hamiltonian H on P determine new reduced trajectories on the reduced space. This new dynamical system is, naturally, called the *reduced system*. The trajectories on the sphere in Figure 4 are the reduced trajectories for the rigid body problem.

We saw that steady rotations of the rigid body correspond to fixed points on the reduced manifold, namely, the body angular momentum sphere in Figure 4. In general, fixed points of the reduced dynamics on P_μ are called *relative equilibria*, following terminology first introduced by Poincaré around 1880. The reduction process can be applied to the system which models the motion of the moon Hyperion, to spinning tops, to fluid and plasma systems, and to systems of coupled rigid bodies. For example, if a system of coupled rigid bodies is undergoing steady rotation, with the internal parts not moving relative to each other, this will be a relative equilibrium of the system. An oblate Earth in steady rotation is a relative equilibrium for a fluid-elastic body. In general, the bigger the symmetry group, the richer the supply of relative equilibria.

Stability

Having discussed the reduction procedure, we turn to the stability of the reduced dynamics. There is a standard procedure for finding the stability of equilibria of an ordinary differential equation

$$\dot{\mathbf{x}} = \mathbf{f}(\mathbf{x})$$

where $\mathbf{x} = (x_1, \ldots, x_n)$ and $\mathbf{f}$ is smooth. The procedure involves solving for the equilibria (fixed points) of the differential equation. These are the points $\mathbf{x}_e$ such that $\mathbf{f}(\mathbf{x}_e) = 0$; i.e., points that are fixed in time under the dynamics. The goal of this procedure is to determine the stability of the fixed point $\mathbf{x}_e$. By stability here we mean that any solution to $\dot{\mathbf{x}} = \mathbf{f}(\mathbf{x})$ that starts near $\mathbf{x}_e$ remains close to $\mathbf{x}_e$ for *all* future time.

A traditional method of ascertaining the stability of $\mathbf{x}_e$ is to examine the first variation equation

$$\dot{\xi} = \mathbf{D}_x\mathbf{f}(\mathbf{x}_e)\xi$$

where $\mathbf{D}_x\mathbf{f}(\mathbf{x}_e)$ is the Jacobian of $\mathbf{f}$ at $\mathbf{x}_e$ and is defined to be the matrix of partial derivatives

$$\mathbf{D}_x\mathbf{f}(\mathbf{x}_e) = \left[\frac{\partial f_i}{\partial x_j}\right]_{x=x_e}$$

The eigenvalues of $\mathbf{D}_x\mathbf{f}(\mathbf{x}_e)$ are then examined. If all the eigenvalues lie in the left half plane, then, by a result of Liapunov [1909], the fixed point is stable. If any of the eigenvalues lie in the right half plane, then the fixed point is unstable. However, for Hamiltonian systems the eigenvalues come in pairs or quartets symmetric about the origin and so they cannot all lie in the left half plane. Thus, this standard stability result will never allow us to deduce whether a Hamiltonian system contains a stable fixed point. As the class of Hamiltonian systems includes the equations which are used to model motions of orbiting space stations and space telescopes, it is imperative to develop explicit conditions to ensure the stability of their orbits.

When the Hamiltonian is in canonical form one can use a stability test for fixed points due to Lagrange and Dirichlet. This method uses the fact that for a fixed point $(\mathbf{q}_e,\mathbf{p}_e)$ of such a system,

$$\frac{\partial H}{\partial q^i}(\mathbf{q}_e,\mathbf{p}_e) = \frac{\partial H}{\partial p_i}(\mathbf{q}_e,\mathbf{p}_e) = 0.$$

Hence, the fixed point occurs at a critical point of the Hamiltonian. If the $2n \times 2n$ matrix $\mathbf{D}^2H$ of second partial derivatives is either positive or negative definite at $(\mathbf{q}_e,\mathbf{p}_e)$ then one has a stable fixed point. Consider the positive definite case. Conceptually, the reason for stability is very simple: since H has a minimum at $(\mathbf{q}_e,\mathbf{p}_e)$ and energy is conserved, solutions stay on level surfaces of H, so that a solution starting near the minimum has to *stay* near the minimum. For a Hamiltonian of the form kinetic plus potential (V), critical points occur when $\mathbf{p}_e = 0$ and $\mathbf{q}_e$ is a critical point of the potential of V. This criterion then reduces to asking for a minimum of V.

In fact, this criterion was used to solve one of the classical problems of the 19th century: the problem of rotating gravitating fluid masses. This problem was studied by Newton, Mac-

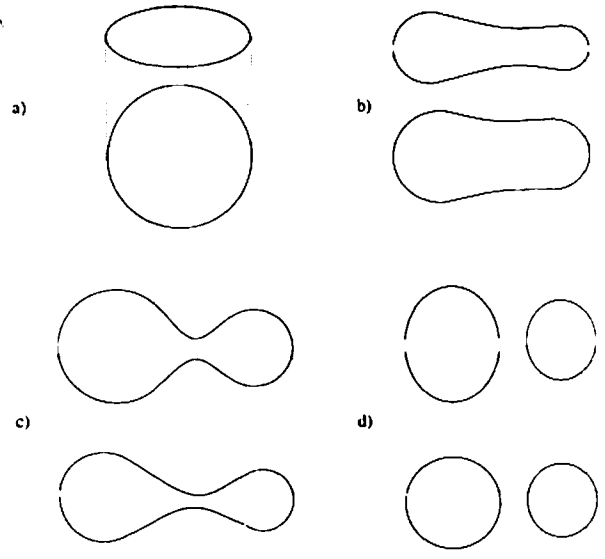

Figure 5: The formation of pear-shaped objects of equilibrium of a rotating fluid mass as it solidifies. Shown are the horizontal and vertical projections of the fluid masses during bifurcation (after Poincaré [1892]).

Laurin, Jacobi, Riemann, Poincaré, and others. The motivation for its study was in the conjectured birth of two planets by the splitting of a large mass of solidifying rotating fluid as shown in Figure 5. This is an example of what has since become known as a *symmetry-breaking bifurcation*. These ideas are important in understanding pattern formation and many of the resulting symmetric objects we see in nature. Poincaré [1892, 1901] was a major contributor to the study of this phenomenon and used the potential energy and angular momentum to deduce the stability and bifurcation of rotating fluids.

The Lagrange-Dirichlet method was generalized by Arnold [1966b] into what has become known as the *energy-Casimir method*. Arnold analyzed the stability of stationary flows of perfect fluids and also developed an explicit stability criterion for the case in which the configuration space for the Hamiltonian of this system is a group which coincides with the symmetry group of the mechanical system. A *Casimir* C is characterized by the fact that it Poisson commutes with *any* function F defined on the phase space of the Hamiltonian system, i.e.,

$$\{C,F\} = 0.$$

(The name Casimir is used in recognition of work by H. B. G. Casimir, who introduced closely related ideas in representation theory.) Large classes of Casimirs usually occur when the reduction procedure is performed, resulting in systems with noncanonical brackets.

For example, in the case of the rigid body discussed previously, if Φ is a function of one variable and Π is the angular momentum vector in the inertial coordinate system, then

$$C(\Pi) = \Phi(\|\Pi\|^2)$$

is a Casimir for the rigid body bracket. The energy-Casimir method involves choosing C such that $H + C$ has a critical point at an equilibrium z_e and then examining $\mathbf{D}^2(H + C)(z_e)$. If this matrix is positive or negative definite then the equilibrium z_e is stable. When the phase space is obtained by reduction, the equilibrium z_e is a relative equilibrium of the original Hamiltonian system.

The energy-Casimir method has been applied to a variety of problems including problems in fluids and plasmas (Holm, Marsden, Ratiu, Weinstein [1985]) and rigid bodies with flexible attachments (Krishnaprasad and Marsden [1987]). If applicable, the energy-Casimir method may permit an explicit determination of the stability of the relative equilibria. It is important to remember, however, that these techniques give stability information only. As such one cannot use them to infer *instability* without further investigation.

The energy-Casimir method is restricted to certain types of systems, since its implementation relies on an abundant supply of Casimir functions. In some important examples, Casimirs have not yet been found and may not even exist. Two methods developed to overcome this difficulty are known as the energy momentum method (EMM) and the reduced energy momentum method (REMM). These two methods are closely linked to the method of reduction. They use conserved quantities, namely the energy and momentum maps, that are usually readily available, rather than Casimirs.

The energy momentum method (Simo, Posbergh and Marsden [1990a,b], Simo, Lewis and Marsden [1990], and Lewis and Simo [1990]) involves the *augmented Hamiltonian* defined by

$$H_\xi = H(q, p) - \xi \cdot J(q, p),$$

where J is the momentum map described in the previous section and ξ may be thought of as a Lagrange multiplier. One then sets the first variation of H_ξ equal to zero to obtain the relative equilibria. To ascertain stability, the second variation $\mathbf{D}^2H_\xi$ is calculated. One is then interested in determining the definiteness of the second variation.

Definiteness in this context has to be properly interpreted to take into account the conservation of the momentum map J and the fact that $\mathbf{D}^2H_\xi$ may have zero eigenvalues due to symmetry. The variations of p and q must satisfy the linearized angular momentum constraint $(\delta q, \delta p) \in \ker[\mathbf{D}J(q_e, p_e)]$, and must not lie in symmetry directions; only these variations are used to calculate the second variation of the augmented Hamiltonian H_ξ. The energy momentum method has been applied to the stability of relative equilibria of among others, coupled rigid bodies and geometrically exact rods (Simo, Posbergh and Marsden [1990a,b] and Patrick [1990]).

Cornerstones in the development of the EMM and REMM were laid by Routh [1877] and Smale [1970], who studied the stability of relative equilibria of simple mechanical systems. Simple mechanical systems are those whose Hamiltonian may be written as the sum of the potential and kinetic energies; the linear harmonic oscillator $\ddot{x} + \omega^2 x = 0$ is an example of such a system. Smale showed that there is a naturally occurring connection that plays an important role in the reduction of a simple mechanical system with symmetry. (A connection can be thought of physically as a generalization of the electromagnetic vector potential, A. See Zwanziger, Koenig, and Pines [1990]). We now call this the *mechanical connection*. Smale also showed that the relative equilibria of these systems are given by the critical points of the *amended potential function* V_{μ_e}, defined below.

The amended potential plays a crucial role in the REMM (see Simo, Lewis and Marsden [1990], and Lewis and Simo [1990]). The REMM exploits properties of the reduction method to put the second variation into a normal form. First one calculates the amended potential V_{μ_e} which is the potential energy of the system plus a generalization of the potential energy of the centrifugal forces in stationary rotation:

$$V_{\mu_e}(q) = V(q) + \frac{1}{2}\mu_e \cdot \mathbb{I}^{-1}(q)\mu_e,$$

where $\mathbb{I}$ is the locked inertia tensor, a generalization of the

inertia tensor of the rigid body obtained by *locking* all the joints in the configuration q. The momentum p_e need not be zero since the system is typically in motion. The second variation directly yields the stability of the relative equilibria. However, an interesting phenomenon occurs if the tangent space $\mathcal{V}$ is split into two specially chosen subspaces $\mathcal{V}_{RIG}$ and $\mathcal{V}_{INT}$ (Simo, Lewis and Marsden [1990]). In this case the second variation block diagonalizes:

$$\mathbf{D}^2V_{\mu_e}|\mathcal{V}\times\mathcal{V} = \begin{bmatrix} \mathbf{D}^2V_{\mu_e}|\,\mathcal{V}_{RIG}\times\mathcal{V}_{RIG} & 0 \\ 0 & \mathbf{D}^2V_{\mu_e}|\,\mathcal{V}_{INT}\times\mathcal{V}_{INT} \end{bmatrix}.$$

The space $\mathcal{V}_{RIG}$ (rotation variations) is generated by the symmetry group, and $\mathcal{V}_{INT}$ are the internal or shape variations. In addition, the whole matrix $\mathbf{D}^2H_\xi$ block diagonalizes in a very efficient manner. This often allows the stability conditions associated with $\mathbf{D}^2V_{\mu_e}|\,\mathcal{V}\times\mathcal{V}$ to recast in terms of a standard eigenvalue problem for the second variation of the amended potential.

This splitting/diagonalization has important computational implications. In the case of pseudo-rigid bodies (Lewis and Simo [1990]), this splitting results in reducing the stability problem to the examination of a single 3×3 matrix instead of a full 18×18 array. (The large matrix becomes diagonal except for a 3×3 subblock on the diagonal.) The block diagonalization approach enabled Lewis and Simo to solve their problem analytically, whereas without it, a substantial numerical computation would have been necessary. The idea of block diagonalization can be taken further. It turns out that $\mathbf{D}^2H_\xi$ and the symplectic structure can be explicitly brought into normal form *simultaneously*. Although investigations are still at an early stage, this result promises to simplify computations in perturbation theory and the study of bifurcation phenomena.

In general, this diagonalization *explicitly separates the rotational and internal modes*, a result which is extremely important not only in rotating and elastic fluid systems, but also in molecular dynamics and robotics. Similar simplifications are expected in the analysis of other problems to be tackled using the reduced energy momentum method.

Appendix A: On the Reduction Construction

In this appendix, we explain a few of the general notions used in the reduction theorem. In the text, we used the example of the free rigid body to illustrate the concept of reduction. The angular momentum space for the rigid body can be interpreted as the dual space of the Lie algebra of $SO(3)$. This is a three dimensional vector space usually identified with $\mathbb{R}^3$. The analogue of the angular momentum space in general reduction theory is $\mathfrak{g}^*$, the dual of the Lie algebra of the symmetry group G.

The momentum map is a map $J: P\to\mathfrak{g}^*$ with the property that, for each $\xi\in\mathfrak{g}$, $\langle J,\xi\rangle$ generates, in the sense of Hamilton's equations, the infinitesimal action in the same way that angular momentum $\mathbf{q}\times\mathbf{p}$ generates rotations. The level set with value $\mu\in\mathfrak{g}^*$ is $J^{-1}(\mu)$, which will be a submanifold of P under certain conditions. The group G_μ is the subgroup of G that maps $J^{-1}(\mu)$ to itself. (It can also be defined as the subgroup that fixes the value μ under the coadjoint action of G on $\mathfrak{g}^*$.) The reduced space is then the quotient $P_\mu = J^{-1}(\mu)/G_\mu$.

Whereas P_μ is symplectic, the manifold P/G is *Poisson* (the bracket of two functions on P/G is defined by regarding them as G-invariant functions on P). If μ is considered as a parameter, one can show that the P_μ are the symplectic leaves in P/G in the same way that the spheres $\|\Pi\| =$ constant are the symplectic leaves in the three dimensional angular momentum space.

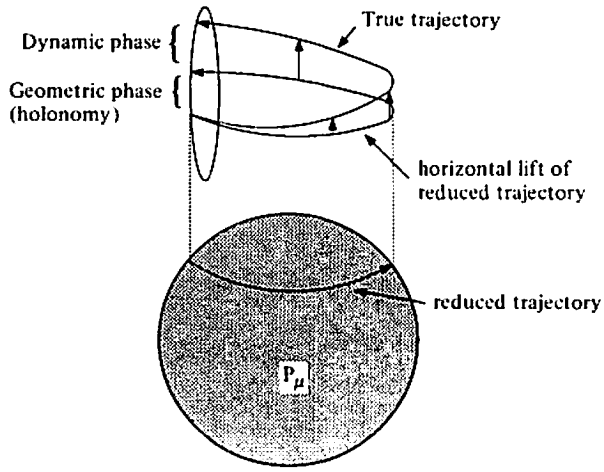

Figure A1: Holonomy for the rigid body (after Marsden, Montgomery, and Ratiu [1990]). As the body completes one period in P_μ, the reduced phase space, the body's true configuration does not return to its original value. The phase difference is equal to the influence of a dynamic phase which takes into account the body's energy, and a geometric phase which depends only on the area of P_μ enclosed by the reduced trajectory.

An important case of the reduction theorem arises when the configuration space is identical to the symmetry group, so that $P = T^*Q = T^*G$. Then the Poisson manifold $P/G = (T^*G)/G$ is identified with the linear space $\mathfrak{g}^*$. This identification induces a special Poisson structure on $\mathfrak{g}^*$ known as the *Lie-Poisson* structure. The Lie-Poisson bracket of two functions F and K on $\mathfrak{g}^*$ is defined by

$$\{F,K\}_\pm(\mu) = \pm\left\langle \mu, \left[\frac{\delta F}{\delta\mu}, \frac{\delta K}{\delta\mu}\right]\right\rangle, \qquad \mu\in\mathfrak{g}^*,$$

where the derivative $\delta F/\delta\mu$ is the usual derivative of F regarded as taking values in $\mathfrak{g}$, and $[,]$ is the Lie bracket on $\mathfrak{g}$. The general Lie-Poisson bracket $\{,\}_\pm$ is the bracket obtained from $(T^*G)/G$ using right multiplication for the plus sign and left multiplication for the minus sign. The rigid body bracket discussed in the text is the special case $G = SO(3)$, using the minus sign in the definition above.

Let us indicate how holonomy is linked closely to the reduction process by returning to our rigid body example. Picture the rigid body as tracing out a path in its phase space $T^*SO(3)$. Conservation of angular momentum implies that the path lies in the submanifold consisting of all points which are mapped onto μ by the momentum map. These points are then mapped to a curve in P_μ by the reduction process; i.e., by the quotient map $J^{-1}(\mu)\to P_\mu$. As Figure 4 in the text shows, almost every trajectory on this reduced space is periodic, but this does *not* imply that the original path was periodic, as is shown in Figure A1. The difference between the true trajectory and a periodic trajectory is given by the holonomy plus the dynamic phase. This is given quantitatively by formula (RBP) in the text and the reduction picture presented here is useful in proving it.

We remark that the reduction construction for the rigid body corresponds to the *Hopf fibration* which describes the three-sphere S^3 as a nontrivial circle bundle over S^2. In our example, S^3 is the subset of phase space which is mapped to μ under the reduction process. (More accurately, $J^{-1}(\mu)$ is $SO(3)\approx S^3/\mathbb{Z}_2$.) See Koçak et al. [1986] or Appendix C for more details.

References

/. Arnold [1966a] Sur la géometric differentielle des groupes de Lie de dimension infinie et ses applications a L'hydrodynamique des fluids parfaits, *Ann. Inst. Fourier. Grenoble*, **16**, 319–361.

V. Arnold [1966b] An a priori estimate in the theory of hydrodynamic stability, *Izv. Vyssh. Uchebn. Zaved. Matematicka*, **54**, 3–5 (in Russian, English Translation in *Amer. Math. Soc. Trans.*, **79**).

M. Berry [1984] Quantal phase factors accompanying adiabatic changes, *Proc. Roy. Soc. London, A*, **392**, 45–57.

M. Berry [1985] Classical adiabatic angles and quantal adiabatic phase, *J. Phys. A: Math. Gen.*, **18**, 15–27.

H. Crabtree [1909] *An Elementary Treatment of the Theory of Spinning Tops and Gyroscopic Motion*, London. Reprinted Chelsea Publishing Company, New York, [1967].

J. Guckenheimer and P. Holmes [1983] *Nonlinear Oscillations, Dynamical Systems, and Bifurcations of Vector Fields*, Springer-Verlag, New York.

J. Hannay [1985] Angle variable holonomy in adiabatic excursion of an integrable Hamiltonian, *J. Phys. A: Math. Gen.*, **18**, 221–230.

J. Hodgins and M. Raibert [1990] Biped gymnastics, *Int. J. Robotics Research*, **9**, 115.

D. Holm, J. Marsden, T. Ratiu and A. Weinstein [1985] Nonlinear stability of fluid and plasma equilibria. *Physics Reports*, **123**, 1–116.

T. Kane and M. Scher [1969] A dynamical explanation of the falling cat phenomenon, *Int. J. Solids Structures*, **5**, 663–670.

P. S. Krishnaprasad and J. E. Marsden [1987] Hamiltonian structure and stability for rigid bodies with flexible attachments, *Arch. Rational Mech. Anal.*, **98**, 71–93.

D. Lewis and J. C. Simo [1990] Nonlinear stability of rotating pseudo-rigid bodies, *Proc. Royal Soc.*, Series A, **427**, 218–239.

J. E. Marsden, A. Weinstein, T. Ratiu, R. Schmid, and R. G. Spencer [1983] Hamiltonian systems with symmetry, coadjoint orbits and plasma physics, *Proc. IUTAM-ISIMM Symposium on "Modern Developments in Analytical Mechanics,"* Torino, June 7–11, 1982, *Atti della Academia della Scienze di Torino* **117**, 289–340.

J. E. Marsden and A. Weinstein [1974] Reduction of symplectic manifolds with symmetry, *Rep. Math. Phys.*, **5**, 121–130.

K. R. Meyer [1973] Symmetries and integrals in mechanics. In *Dynamical systems*, M. Peixoto (ed.), Academic Press, 259–273.

R. Montgomery [1990] Isoholonomic problems and some applications, *Comm. Math. Phys.*, **128**, 565–592.

Nature [1894] Photographs of a tumbling cat. **51**, 80–81.

G. Patrick [1990] Dynamics of coupled rigid bodies, thesis, Berkeley (see also *Cont. Math. AMS*, **97**, 1989).

H. Poincaré [1892] Les formes d'equilibre d'une masse fluide en rotation, *Revue Génèrale des Sciences*, **3**, 809–815.

H. Poincaré [1901] Sur la stabilité de l'équilibre des figures piriformes affectées par une masse fluide en rotation, *Philosophical Transactions A*, **198**, 333–373.

E. J. Routh [1877] Stability of a given state of motion, reprinted in *Stability of Motion*, ed. A. T. Fuller, Halsted Press, New York, 1975.

J. C. Simo, D. Lewis and J. E. Marsden [1990] The stability of relative equilibria. Part I: The reduced energy momentum method *Arch. Rational Mech. Anal* (to appear).

J. C. Simo, T. A. Posbergh, and J. E. Marsden [1990a] Stability of coupled rigid body and geometrically exact rods: Block diagonalization and the energy-momentum method. *Physics Reports*, **193**, 279–360.

J. C. Simo, T. A. Posbergh and J. E. Marsden [1990b] The stability of relative equilibria. Part II: Application to nonlinear elasticity, *Arch. Rational Mech. Anal* (to appear).

S. Smale [1970] Topology and mechanics, *Inventions Math.*, **10**, 305–331.

J. N. Wilford [1990] Troubles continue to plague orbiting Hubble telescope, *New York Times*, June 15, 16A.

J. Wisdom, S. J. Peale, and F. Mignard [1984] The chaotic rotation of Hyperion, *Icarus*, **58**, 137–152.

I. W. Zwanziger, M. Koenig, and A. Pines [1990] Berry's phase, *Annu. Rev. Phys. Chem.*, **41**, 601–646.

Part II in next issue

Symmetry, Stability, Geometric Phases, and Mechanical Integrators (Part II)

J. E. Marsden, O. M. O'Reilly†, F. J. Wicklin‡, B. W. Zombro§*

[Part I of this paper appeared in *NLST* 1:1, pp. 4–11.]

Geometric Phases

The application of the methods described in Part I is still in its infancy, but the previous example clearly indicates the power of reduction and suggests that the REMM will be applied to dynamic problems in many fields, including chemistry, quantum and classical physics, and engineering. Apart from the computational simplification afforded by reduction, reduction also permits us to put into a mechanical context a concept known as the geometric phase, or *holonomy*.

A well-known example of holonomy is the Foucault pendulum. During a single rotation of the earth, the plane of the pendulum's oscillations is shifted by an angle which depends only on the latitude of the pendulum's location. Specifically, if a pendulum located at latitude α is swinging in a plane, then after twenty-four hours, the plane of its oscillations will have shifted by an angle of $-2\pi \sin \alpha$. This holonomy is a result of parallel translation: if an orthonormal coordinate frame undergoes parallel transport along a line of latitude α, then after one revolution the frame will have rotated by an amount equal to the phase shift of the the Foucault pendulum. (See Figure 6.)

Geometrically, the holonomy of the Foucault pendulum is equal to the solid angle swept out by the pendulum's axis during one rotation of the earth. Thus a pendulum at the north pole of the earth will experience a holonomy of -2π, whereas a pendulum on the earth's equator experiences no holonomy. Both of these results are with respect to the laboratory frame.

A less familiar example of holonomy was presented by Hannay [1985] and discussed further by Berry [1985, 1988]. Consider a frictionless, *non*-circular, planar hoop of wire on which is placed a small bead. The bead is set in motion and allowed to slide along the wire at a constant speed. Clearly the bead will return to its initial position after, say, T seconds, and will continue to return every T seconds after that. Suppose however, that the wire hoop is slowly rotated in its plane by 360 degrees while the bead is in motion. At the end of the rotation, the bead is *not* in the location where we might expect it, but instead will be found at a shifted position which is completely determined by the shape of the hoop. In fact, the shift in position depends only on the length of the hoop, L, and on the area it encloses, A. The shift is approximately given by $8\pi^2 A/L^2$ as an angle, or by $4\pi A/L$ as length. (See Hannay [1985] or Marsden, Montgomery, and Ratiu [1990] for a derivation of these formulas.) To be completely concrete, if the bead's initial position is marked with a tick and if the time of rotation is a multiple of the bead's period, then at the end of rotation the bead is found $4\pi A/L$ units from its initial position. This is shown in Figure 7. We remark that if the hoop is circular then the angular shift is 2π and so the holonomy is not observable.

There is a similar explicit formula for the freely rotating rigid body. Suppose that a rigid body has spatial angular momentum given by the vector μ and has total energy E given by (RBH). If the (reduced) trajectory on the angular momentum sphere (Figure 4) is periodic with period T then the trajectory must enclose some surface area, S on this sphere. A formula of Montgomery's (see,

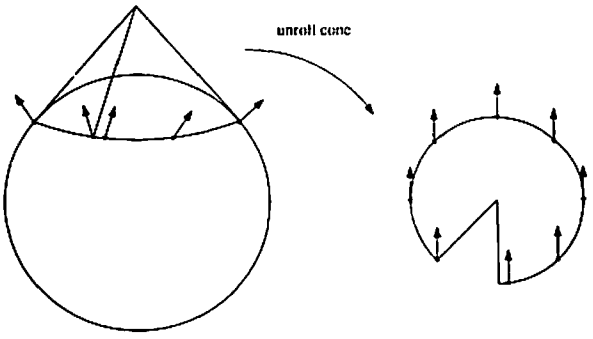

Figure 6: The parallel transport of a coordinate frame along a curved surface (after Arnold [1978]).

*Department of Mathematics, University of California, Berkeley, CA 94720.
†Department of Theoretical and Applied Mechanics, Cornell University, Ithaca, NY 14853. Research partially supported by NSF Grant DMS-8703656.
‡Center for Applied Mathematics, Cornell University, Ithaca, NY 14853. Research partially supported by NSF Graduate Fellowship.
§Department of Theoretical and Applied Mechanics, Cornell University, Ithaca, NY 14853.

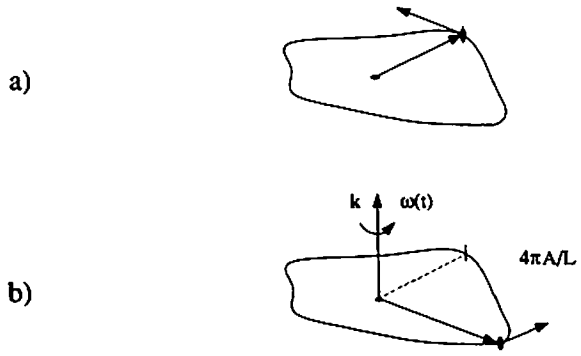

Figure 7: A bead sliding on a planar, non-circular hoop of area A and length L. In a), the bead slides around the hoop at constant speed with period T. In b), the hoop is slowly rotated through 360 degrees. After one rotation, the bead is located $4\pi A/L$ units behind where it would have been had the rotation not occurred. Shown is the case where the time of rotation is a multiple of T.

for example, Marsden, Montgomery, and Ratiu [1990]) states that after time T the rigid body has rotated (modulo 2π) about the vector μ by the phase angle

$$\Delta\theta = \frac{1}{\|\mu\|}\left\{-\frac{S}{\|\mu\|} + 2ET\right\}. \qquad \text{(RBP)}$$

The approximate phase formula for the ball in the hoop is derived by the classical techniques of averaging and the variation of constants formula. However, formula (RBP) is *exact* and requires geometric methods to prove.

The interesting feature of (RBP) is that $\Delta\theta$ is split into two parts. The first term is purely geometric and so is called the *geometric phase*. It does not depend on the energy of the system or the period of motion, but rather on the fraction of the surface area of the angular momentum sphere which is enclosed by the periodic trajectory. Since we allow A to be either of the two areas "enclosed" by the trajectory, the result obtained is valid up to the addition of a multiple of 2π. The geometric phase for classical mechanical systems was first identified by Hannay [1985] (motivated by Berry [1985]) and so it is sometimes called *Hannay's angle* or the *Hannay-Berry phase*. The second term in (RPB) is known as the *dynamic phase* and depends explicitly on the system's energy and the period of the reduced trajectory.

It is possible to observe the holonomy of a rigid body with a simple experiment. Put a rubber band around a book so that the cover will not open. (A "tall," thin book works best.) With the front cover pointing up, gently toss the book in the air so that it rotates about its middle axis, as shown in Figure 8. Catch the book after a single rotation and you will find that it has *also* rotated by 180 degrees about its long axis—that is, the front cover is now facing the floor! (Cushman and others have given a careful analysis of this problem.)

There are further examples of familiar everyday occurrences which demonstrate holonomy. We have already mentioned the fact that a falling cat often manages to land upright, and can even accomplish this feat if released while upside down with total angular momentum zero. Montgomery [1990] treated the cat as a deformable body and characterized the deformations which allow a cat to reorient itself without violating conservation of angular momentum. In showing that such deformations are possible, Montgomery casts the falling cat problem into geometric language. Let the *shape* of a cat refer to the location of the cat's body parts relative to each other, but without regard to the cat's orientation in space. Let the *configuration* of a cat refer both to the cat's shape and to its orientation with respect to some fixed reference frame. More precisely, if Q is the configuration space and G is the group of rigid motions, then Q/G is the shape space.

For example, if the cat is completely rigid then it will always have the same shape, but we can give it a different configuration by rotating it through, say, 180 degrees about some axis. If we require that the cat have the same shape at the end of its fall as it had at the beginning, then the cat problem may be formulated as follows: Given an initial configuration, what is the most efficient way for a cat to achieve a desired final configuration if the final shape is required to be the same as the initial shape? It turns out that the solution of the falling cat problem is closely related to Wong's equations, which describe the motion of a particle in a Yang-Mills field (Montgomery [1990], Wilczek [1988], and Shapere [1989]).

Geometrically, the picture for the falling cat problem is analogous to that presented earlier for a rigid body. We think of the cat as tracing out some path in configuration space during its fall. The projection of this path onto the shape space results in a trajectory in the shape space, and the requirement that the cat's initial and final shapes are the same means that the trajectory is a closed loop. Furthermore, if we want to know the most efficient configuration path which satisfies the initial and final conditions, then we want to find the shortest path with respect to a metric induced by the function we wish to minimize.

Intuitively, we may define holonomy as a difference between the initial and final configuration of a system which results from a cyclic change of the system's shape. A simple example (due to Cherry [1989] and shown in Figure 9) is to stand with your arms at your side, your palm facing forward, and your thumb facing out. Keeping your arm straight, lift your arm sideways until it is

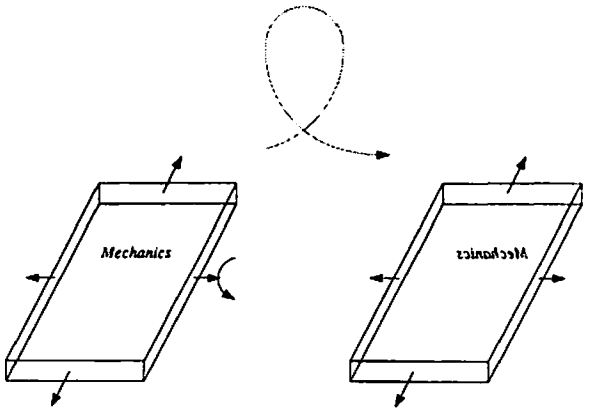

Figure 8: A book tossed in the air about an axis which is close to middle (unstable) axis experiences a holonomy of 180 degrees about its long axis when caught after one revolution.

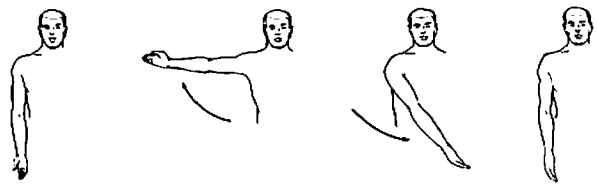

Figure 9: An example of holonomy. Although the arm completes a cycle in its shape space, there is a 90 degree rotation in the configuration space.

parallel to the floor, then, keeping your thumb up, swing your arm forward until your fingers point straight ahead. Now return your arm to your side and you will find that your palm faces inwards and your thumb points forward—a 90 degree change in the configuration of your arm! Note again that the holonomy does not depend on the length of your arm, nor on its mass, nor on how quickly you perform the actions; the holonomy is a purely geometric result. Expressed slightly differently, the geometric phase is independent of a particular parametrization, whereas the dynamic phase may be parametrization dependent.

The examples above indicate that holonomic occurrences are not rare. In fact, Shapere and Wilczek [1987] showed that aquatic microorganisms use holonomy as a form of propulsion. Because these organisms are so small, the environment in which they live is extremely viscous to them. The apparent viscosity is so great, in fact, that they are unable to swim by conventional stroking motions, just as a person trapped in a tar pit would be unable to swim to safety. These microorganisms surmount their locomotion difficulties, however, by moving their "tails" or changing their shapes in a topologically nontrivial way which induces a holonomy and allows them to move forward through their environment. There are probably many consequences and applications of this observation that remain to be discovered. It is tempting to use the phrase *holonomy drive* for any process in which holonomy is used to effect a change of position.

Yang and Krishnaprasad [1990] have provided an example of holonomy drive for coupled rigid bodies linked together with pivot joints as shown in Figure 10. (For simplicity, the bodies are represented as rigid rods.) This form of linkage permits the rods to freely rotate with respect to each other, and we assume that the system is not subjected to external forces or torques, although torques will exist in the joints as the assemblage rotates. By our assumptions, angular momentum is conserved in this system. Yet, even if the total angular momentum is zero, a turn of the crank (as indicated in Figure 10) returns the system to its initial shape but creates a holonomy which rotates the system's configuration. See Thurston and Weeks [1986] for some relationships between linkages and the theory of 3-manifolds.

It is natural to ask, is there a way for humans to exploit holonomy drive to our advantage? Scientists in a variety of fields are already exploring this question. Panasonic has developed a "micromotor" which can focus a camera lens using the principle of holonomy. A qualitative explanation of such a micromotor is

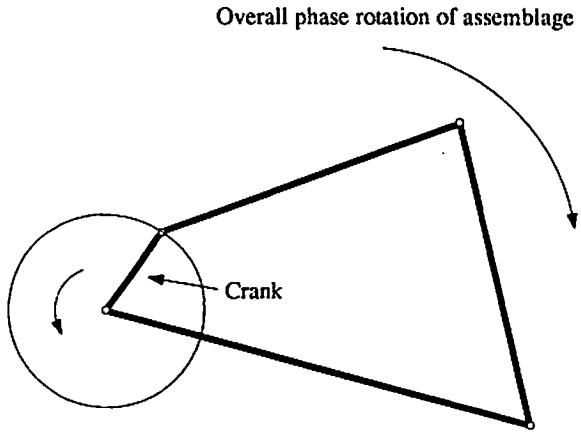

Figure 10: Rigid rods linked by pivot joints. As the "crank" traces out the path shown, the assemblage experiences a holonomy resulting in a clockwise shift in its configuration. Figure provided by P. S. Krishnaprasad.

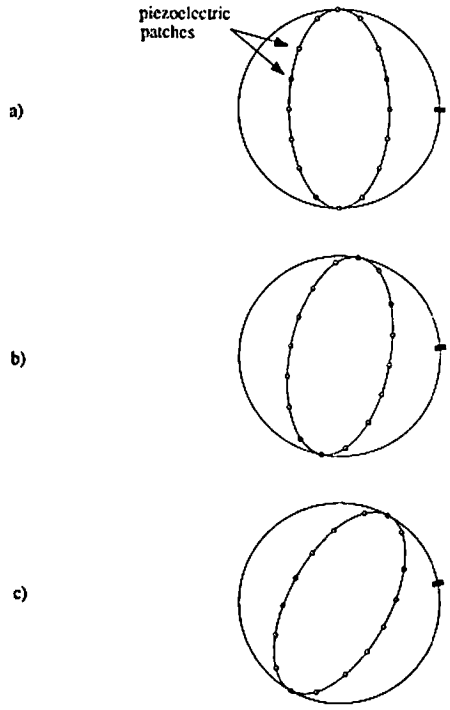

Figure 11: Example of a motor which utilizes holonomy. a) Piezoelastic patches send signals to a flexible inner ring which deforms so that it touches a rigid external ring. b) A second set of signals deforms the inner ring along a direction which is slightly offset from the first direction. c) As this process is continued, the external ring rotates retrograde to the perceived motion of the inner ring.

presented in Ise [1986].

Brockett [1987, 1989] is also exploring the feasibility of holonomic motors. An example of the holonomic motor principle is shown in Figure 11. A flexible inner ring is concentrically placed inside a rigid outer ring. A computer controls piezoelectric patches which are attached to the inner ring and are used to deform the inner ring along some predetermined axis. The axis of deformation is slowly rotated (say, clockwise) from one deformation to the next. It is important to note that the inner ring *does not rotate*, but is merely being deformed in a different direction at each step. The net result of these actions is that the outer ring *rotates* in a direction which is retrograde to the rotation of the axis of deformation (in our case, counter-clockwise). If we imagine the outer ring being connected, for example, to some axle, then we see how this process naturally produces a motor. An extension of this work may even produce a "spherical" motor in which a flexible sphere is concentrically placed within a slightly larger outer sphere. Transverse bands of piezoelectric patches working in synchrony could then be used to rotate the outer sphere *in any direction*.

Holonomy may be important in the field of magnetic resonance imaging (MRI) and spectroscopy. Theoretical work by Berry [1984, 1988] has shown that if a quantum system experiences a slow (adiabatic) cyclic change, then there will be a shift in the phase of the system's wave function. This is a quantum analogue to the bead on a hoop problem discussed above. This work has been verified by several independent experiments; the implications of this result to MRI and spectroscopy are still being investigated. For a review of the applications of geometric phase to the

fields of spectroscopy, field theory, and solid-state physics, see Zwanziger, Koenig, and Pines [1990] and the extensive bibliography therein.

Yet another possible application of holonomy drive is the somersaulting robot. Due to the finite precision response of motors and actuators, a slight error in the robot's initial angular momentum can result in an unsatsifactory landing as the robot attempts a flip. Yet, in spite of the challenges, Hodgins and Raibert [1989] report that the robot can currently execute 90 percent of the flips successfully. Montgomery, Raibert, and Li [1990] are asking whether a robot can use holonomy to improve this rate of success. To do this, they reformulate the falling cat problem as a problem in feedback control: the cat must use information gained by its senses in order to determine how to twist and turn its body so that it successfully lands on its feet.

It is possible that the same technique used by cats can be implemented in a robot which also wants to complete a flip in mid-air. Imagine a robot installed with sensors so that as it begins its somersault it measures its momenta (linear and angular) and quickly calculates its final landing position. If the calculated final configuration is different from the intended final configuration, then the robot waves mechanical arms and legs *while entirely in the air* to create a holonomy which equals the difference between the two configurations.

If holonomy drive can be used to control a mechanical structure, then there may be profound implications for future orbiting space telescopes. Suppose a telescope initially has zero angular momentum (with respect to its orbital frame), and suppose it needs to be turned 180 degrees. One way to do this is to fire a small jet which would give it angular momentum, then, when the turn is nearly complete, fire a second jet which acts as a brake to exactly cancel the angular momentum. As in the somersaulting robot, however, errors are bound to occur, and the process of returning the telescope to (approximately) zero angular momentum may be a long process. It would seem to be more desirable to turn it *while constantly preserving zero angular momentum*. The falling cat performs this very trick.

Teaching a robot to utilize holonomy drive may be possible, but if this feedback process is to work, the robot must be able to make an accurate prediction of its final configuration based on data provided by its sensors. More importantly, these predictions must be made fast enough that the robot can compute and implement a holonomic series of motions while still in the air.

Mechanical Integrators

The development of fast and accurate numerical integration techniques has long been a goal in robotics, control theory, space mechanics, and other fields in which the equations of motion must be integrated numerically. For mechanical systems with symmetries, it seems desirable that the numerical algorithms preserve the values of any integrals of motion of the system (for example, energy and angular momentum in the case of the free rigid body), so that the effect of iterating the algorithm is consistent with the reduction of the dynamics in the sense described earlier. There are various approaches to the problem of deriving conservative algorithms, depending, among other factors, on the choice of a particular quantity or quantities that the algorithm is designed to conserve.

A number of algorithms have been developed specifically for integrating Hamiltonian systems to conserve the energy integral, but without attempting to capture all of the details of the Hamiltonian structure (for example, Chorin, Hughes, Marsden, and McCracken [1978], Stofer [1987], Greenspan [1974, 1984], Xie [1990]). Although such algorithms may be constrained to preserve some other integrals of motion as well, they do not *in general* conserve all of the integrals of motion. Thus, for a system which has the energy and several momentum-like quantities as integrals of motion, an energy-conservative algorithm would not be expected to conserve all of the momentum integrals. In fact, some of the standard energy-conservative algorithms have poor momentum behavior over even moderate time ranges. This makes them unsuitable for problems where the exact conservation of a momentum integral is essential to the control mechanism.

Simo and Wong [1989], for example, document instances of angular momentum drift in energy-conservative simulations of certain forced rigid body motions. To control such drifts and attain the high levels of computational accuracy demanded by automated control mechanisms, one would be forced to reduce computational step sizes to such an extent that the numerical simulation would be prohibitively inefficient. A particularly dramatic example of this has been reported by Simo [1990]. According to one of his studies, attempting to simulate both the rotational and vibrational modes of a freely moving rod using a standard energy-conservative algorithm may result in the prediction that the rotational motion will come to a virtual halt after only a few cycles!

If conservation of momentum is more important in a given application than conservation of energy, one would like to be able to generate an appropriate numerical algorithm which exactly conserves momentum (or, more generally, all momentum-like integrals of motion). Of course, numerical anomalies such as angular momentum drift are not always due to inaccuracies in the algorithm. There may be other reasons for failing to get correct answers. For example, it is not obvious how to account for centrifugal and Coriolis forces in a model of a rapidly rotating and flexing beam. This and several other questions involving the modelling of flexible structures have recently been addressed by Simo and Vu-Quoc [1987] and Baillieul and Levi [1987]. Eliminating numerical sources of momentum drift in computations based on particular models makes it easier to evaluate the models themselves.

As we have seen, momentum integrals in Hamiltonian systems are associated with invariance of the system under the action of symmetry groups. Consequently, one might derive momentum-conservative algorithms by constraining the algorithm to obey, in some sense, the same group invariance as the actual dynamics. There is a natural way to accomplish this by exploiting the Hamiltonian structure, and demanding preservation of the symplectic structure as well. This is the context of *symplectic integrators* (originally by De Vogelaére [1956]; see Ge and Marsden [1988] and references therein).

A symplectic integrator is an evolutionary finite-difference algorithm which has the property that each iteration is given by a canonical transformation (also known as a symplectic transformation) of the phase space. The time-step size Δt is a parameter in the symplectic mapping defining the algorithm, so if this mapping approximates the Δt-time map of a particular Hamiltonian flow to at least positive order in Δt, the algorithm may be said to provide a finite-difference approximation of the dynamics in the usual sense. Since any number of iterations of the algorithm still results in a symplectic map, a symplectic integrator also preserves the Hamiltonian structure of the dynamics.

Suppose we are interested in simulating the dynamics of a Hamiltonian system that is invariant under the action of a Lie group G. As discussed previously, we expect such a system to have conserved integrals of motion arising from the momentum map $J : P \to \mathfrak{g}^*$ where P is the phase space. Ge and Marsden [1988] have shown that under fairly weak additional assumptions, a G-equivariant symplectic integrator exactly conserves J, and consequently, *all* integrals of motion associated with the reduction of the dynamics. For example, a symplectic integrator of this type applied to a free rigid body motion would exactly

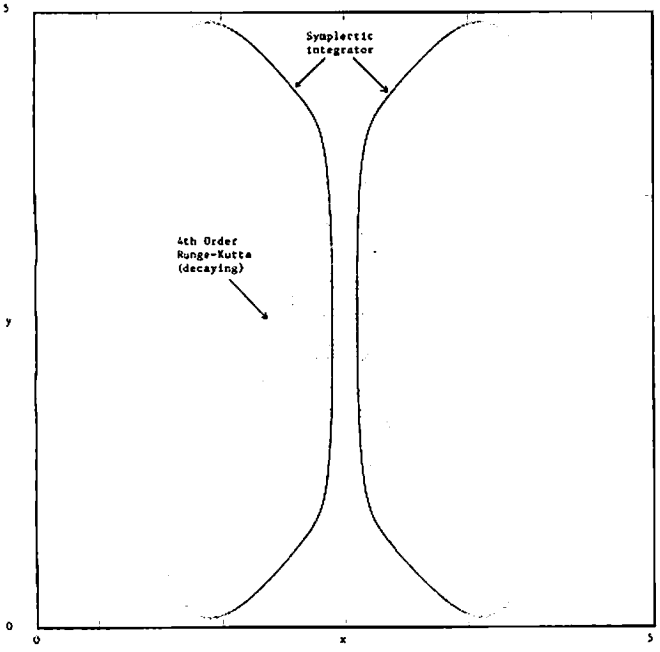

Figure 12: Transverse Poincaré section. A comparison of symplectic versus non-symplectic algorithms. The outermost rings are periodic orbits of a Hamiltonian system as computed with a fourth-order symplectic algorithm. Inside this ring is an orbit computed by fourth-order Runge-Kutta. This orbit appears to decay and spiral inwards, even though both orbits are computed from the same initial condition. The step size in both cases is 0.1. Figure provided by S. Kim.

preserve the initial value of the angular momentum vector in space. More generally, the invariance properties of the algorithm insure that the computed solution will always remain on the reduced phase space of the actual dynamics.

For the important case $P = T^*Q$ with G acting by a cotangent lift, a formula for the mapping defining the algorithm can be obtained conveniently by means of the Hamilton-Jacobi generating function $S_{\Delta t}(q,Q)$. Let $S_{\Delta t}$ be a G-invariant function which approximates the solution of the time-dependent Hamilton-Jacobi equation with Δt representing time. By G-invariant we mean that $S_{\Delta t}(gq, gQ) = S_{\Delta t}(q,Q)$ where g designates the action. Then the associated symplectic map $\phi_{\Delta t} : (q, p) \to (Q, P)$, defined implicitly by the equations

$$p = -\partial S_{\Delta t}/\partial q, \qquad P = \partial S_{\Delta t}/\partial Q,$$

defines a symplectic integrator with the desired conservation properties. A simple example of a first-order symplectic scheme for $H = p^2/2 + V(q)$ is $(q, p) \mapsto (Q, P)$, where

$$Q = q + (\Delta t)p,$$
$$P = p - (\Delta t)\frac{\partial V}{\partial q}(q + (\Delta t)p).$$

This approximate generating function leads to a computationally explicit first-order symplectic algorithm. Using a similar approximate solution, Ge and Marsden [1988] provide an explicit construction of a symplectic integrator for the free rigid body.

Figures 12 and 13 illustrate characteristics of a symplectic integrator (4th order) as compared to a popular conventional algorithm (4th order Runge-Kutta) with comparable pointwise accuracy per iteration. The system being studied is a two degree of freedom Hamiltonian system which has been used to model certain types of surface waves in fluids (Armbruster, Guckenheimer, and Kim [1989]). In Figures 12 and 13 we consider a special case

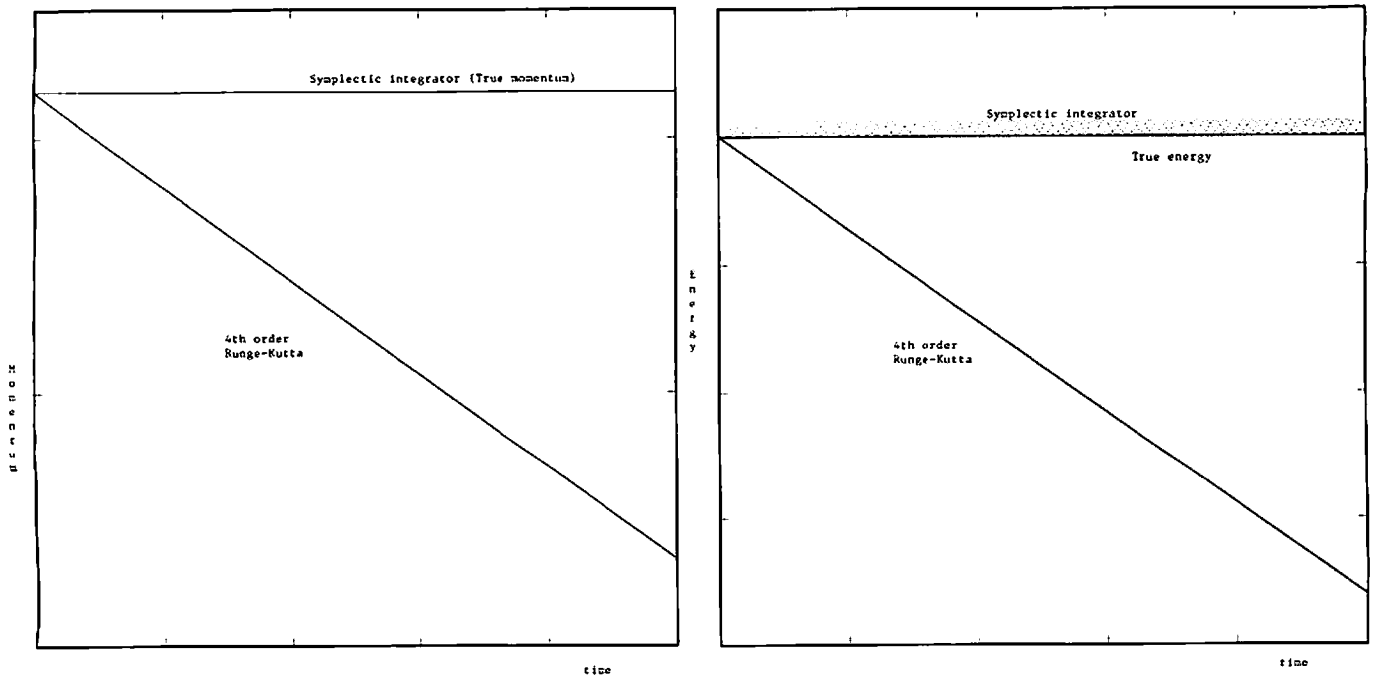

Figure 13: Comparison of fourth order integrators. a) The momentum error of a conventional algorithm may accumulate monotonically in time. b) The Hamiltonian computed by a symplectic integrator typically undergoes bounded oscillations in time. Figure provided by S. Kim.

where the system has a conserved momentum integral. Figure 12 shows a Poincaré section transverse to the appropriate level set of this momentum integral. The Poincaré map computed by the symplectic integrator produces iterates lying entirely on the level set of momentum, whereas there is significant deviation from the level set for the non-symplectic algorithm. Furthermore, the momentum error of the conventional algorithm appears to accumulate monotonically in time, as shown in Figure 13. The possibility of extending the momentum-conservative algorithms to dissipative systems with internal friction which conserve momentum (but not energy) such as orbiting space telescopes should be the subject of further investigations.

Although symplectic integrators do not in general conserve the energy (Hamiltonian) of a mechanical system, there is some numerical evidence that that energy invariance remains in a reasonable range over long time intervals. In fact, it is typically observed that the numerically computed Hamiltonian for a symplectic integrator undergoes *bounded* oscillations in time, whereas conventional algorithms typically produce accumulating energy errors as shown in Figure 13. Channell and Scovel [1990] report other instances of this behavior.

The properties of symplectic integrators also make them highly suitable for long-time integration of chaotic Hamiltonian systems. Figure 14 depicts a numerically computed Poincaré map for the same two degree of freedom system mentioned above, this time slightly perturbed from the integrable limit. This figure was generated by a fourth order symplectic algorithm and exhibits the intermingling of stochastic and regular behavior characteristic of nearly integrable systems. Conventional algorithms require smaller time steps to produce a comparable degree of clarity and may also introduce artificial dissipative effects.

Given the importance of conserving integrals of motion and the important role played by the Hamiltonian structure in the reduction procedure for a system with symmetry, one might hope to find an algorithm which combines *all* of the desirable properties of the symplectic and energy-conservative algorithms: conservation of energy, conservation of momenta (and other independent integrals), and conservation of the symplectic structure. However, according to an argument of Ge [1988], any algorithm having all of these properties must represent the *exact* solution of the original dynamics problem up to a time reparameterization.

Ge's argument is straightforward. Suppose $\phi_{\Delta t}$ is a symplectic algorithm of the type discussed above, and consider the application of the algorithm to the *reduced* phase space. We assume that the Hamiltonian H is the only integral of motion of the reduced dynamics (i.e., all other integrals of the system have been found and taken out in the reduction process). Since $\phi_{\Delta t}$ is symplectic it must be the Δt-time map of some time-dependent Hamiltonian function F. Now assume that the symplectic map $\phi_{\Delta t}$ also conserves H for all values of Δt. Thus $\{H, F\} = 0 = \{F, H\}$. The latter equation implies that F is functionally dependent on H since the flow of H (the "true dynamics") has no other integrals of motion. The functional dependence of F on H in turn implies that their Hamiltonian vector fields are parallel, so the flow of F (the approximate solution) and the flow of H (the exact solution) must lie along identical curves in the reduced phase space; thus the flows are equivalent up to time reparametrization.

This result, succinctly stated, says that *it is impossible for an algorithm to simultaneously conserve the symplectic structure, the momentum map, and the Hamiltonian.* Non-symplectic algorithms that conserve both momentum and energy have recently been studied by Simo and Wong [1989] and Krishnaprasad and Austin [1990]. Their work shows that it is indeed possible to design algorithms of this sort—the ideas are discussed in Appendix B.

In summary, by incorporating the momentum map conservation condition into the *derivation* of the algorithm, one obtains a large class of integrators, some of which also possess other desirable properties. One then has the option of making secondary design choices from among these properties. For example, one may choose whether the integrator will be explicit or implicit, or whether the integrator will conserve energy or symplectic structure. It is not presently clear which options should be preferred for a given application. Recent research has given high priority to the conservation of the momentum map. For the reader interested in the technical details, we have included a mathematical appendix showing how momentum map conservation can be accomplished for a class of symplectic integrators. We also discuss how one might design algorithms conserving the energy and the momentum map.

Conclusions

This article has been a brief survey, and many technical details have been omitted or sketched, but we have attempted to indicate some of the advantages afforded by techniques such as reduction, holonomy, energy-momentum stability tests, and symplectic integration. The recent developments in mechanics presented in this article have applications ranging from micromotors to space stations. They are helping us to understand the locomotion of swimming microorganisms and somersaulting robots. In fact, it is almost a misnomer to classify these developments as belonging solely to the field of mechanics, since the increased understanding of stability, holonomy, and the reduction of dynamics has contributed to developments in robotics, quantum chemistry, magnetic resonance imaging, and microbiology. The success of the techniques described in this paper indicates that fundamental insights into these problems may be obtained by adopting a modern and geometric approach to classical mechanics.

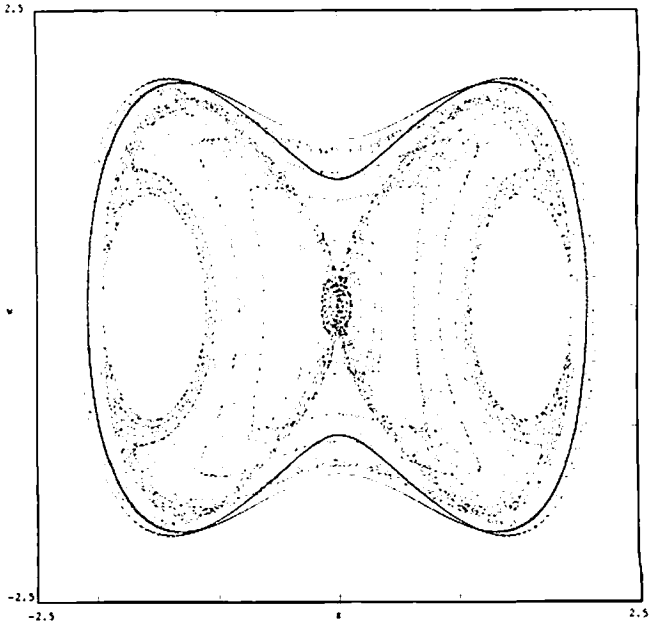

Figure 14: A Poincaré section for a near-integrable Hamiltonian system showing two orbits on the $H = 0$ energy surface. The orbits were computed with a fourth-order symplectic algorithm (Forest-Berz). For the parameter values generating this section, the system behaves like two weakly coupled Duffing oscillators. Armbruster, Guckenheimer, and Kim [1989] have shown that this system contains chaotic trajectories.

Appendix B: Integrators which Preserve Momentum Maps

The construction of momentum-conserving algorithms, whether of symplectic or energy-momentum type, requires that level sets of the momentum map J remain invariant under the mapping $\phi : P \to P$ which represents a single iteration of the algorithm. The geometry of the reduction procedure thus plays a crucial role in both cases. We present here sufficient conditions under which it is possible to obtain such a mapping in the symplectic case. Our argument leads to a simple recipe for deriving the algorithm from an appropriate generating function. We then outline a general procedure for constructing energy-momentum conserving algorithms.

Symplectic Algorithms

The argument is a modification of some ideas found in Ge and Marsden [1988]. The notation is that of Abraham and Marsden [1978]. We make the following assumptions at the outset, which basically define the setting in which reduced symplectic integrators are applicable:

(1) P is a symplectic manifold with an exact symplectic form $\omega = -d\theta$;

(2) G is a Lie group acting symplectically on P and $J : P \to \mathfrak{g}^*$ is an associated momentum map for the action, with g representing the action of an individual element of G;

(3) $\phi : P \to P$ is a symplectic map;

(4) ϕ is G-equivariant: $\phi(gz) = g\phi(z)$, for all $z \in P$.

Letting $\xi_P = X_{\langle J,\xi\rangle}$ designate the vector field corresponding to $\xi \in \mathfrak{g}$ under the action, we start by differentiating the equivariance condition (4)

$$\phi g = g\phi$$

with respect to the group element in the direction of ξ_P at the identity of the group. That is, we take the time derivative of $\phi(g_\xi^t z) = g_\xi^t \phi(z)$, where g_ξ^t is the flow of ξ_P. This results in

$$\phi^* X_{\langle J,\xi\rangle} = X_{\langle J,\xi\rangle}.$$

However, $\phi^* X_{\langle J,\xi\rangle} = X_{\langle J,\xi\rangle \circ \phi}$ as a result of the symplectic condition on ϕ (assumption 3); thus we have

$$X_{\langle J,\xi\rangle \circ \phi} = X_{\langle J,\xi\rangle}.$$

Two Hamiltonian vector fields are equal if and only if their Hamiltonians differ by a constant; therefore we obtain finally

$$\langle J,\xi\rangle \circ \phi - \langle J,\xi\rangle = \text{constant}.$$

We need $\langle J,\xi\rangle \circ \phi = \langle J,\xi\rangle$ for the value of J to be preserved by the map ϕ, so we need to establish sufficient conditions under which the constant will vanish.

We make the following further assumptions:

(*i*) $S : P \to \mathbb{R}$ is a G-invariant generating function for the map ϕ, i.e., $S(gz) = S(z)$ and $\phi^*\theta = \theta + dS$;

(*ii*) $\langle J,\xi\rangle = i_{\xi_P}\theta$.

Now,

$$\begin{aligned}\langle J,\xi\rangle \circ \phi &= \phi^*\langle J,\xi\rangle \\ &= \phi^* i_{\xi_P}\theta \quad \text{(by } ii\text{)} \\ &= i_{\xi_P}\phi^*\theta \quad \text{(by equivariance of } \phi\text{)} \\ &= i_{\xi_P}\theta + i_{\xi_P} dS \quad \text{(by } i\text{)}.\end{aligned}$$

The first term in this last expression is just $\langle J,\xi\rangle$ again, and the final term vanishes by invariance of S. Thus, the desired conservation condition, $\langle J,\xi\rangle \circ \phi = \langle J,\xi\rangle$, follows from assumptions 1–4 and *i* and *ii*.

The additional assumptions *i* and *ii* are not very restrictive in the context of typical applications to mechanics problems. Assuming that the original system is given in terms of canonical coordinates on a cotangent bundle $P = T^*Q$, we have $\omega = -d\theta_0$, where $\theta_0 = pdq$ is the canonical one-form on the cotangent bundle. If the symmetry group G acts by cotangent lifts, then *ii* follows automatically. We may interpret condition *i* as providing a recipe for creating symplectic integrators. Suppose that we can find a G-equivariant function S which approximately generates the flow of the Hamiltonian vector field. Then the algorithm ϕ is given implicitly by the generating relation $\phi^*\theta = \theta + dS$, and so *it will automatically be a momentum preserving symplectic map*.

Energy-Momentum Algorithms

We now turn to the case of constructing an algorithm which conserves the Hamiltonian and the momentum map, but which will not, in general, conserve the symplectic structure.

A class of algorithms satisfying this requirement can be obtained through the steps outlined below.

(1) Formulate any energy-preserving algorithm on the reduced phase space $P_\mu = J^{-1}(\mu)/G_\mu$. A variety of algorithms are readily available, see references cited in Ge and Marsden [1988]. If such an algorithm is interpreted in terms of the primitive phase space P, it is abstractly given as an iterative mapping from one G_μ-orbit in $J^{-1}(\mu)$ to another.

(2) In terms of canonical coordinates (q,p) on P, implement the orbit-to-orbit mapping described above by imposing the constraint $J(q_k, p_k) = J(q_{k+1}, p_{k+1})$. The constraint does not uniquely determine the algorithm on P, so we may obtain a large class of iterative schemes.

(3) To uniquely determine a map from within the above class, we must determine how points in one G_μ-orbit are mapped to points in another orbit. There is still an ambiguity about how phase space points drift in the G_μ-orbit directions. This drift is closely connected with geometric phases! In fact by discretizing the geometric phase formula for the system under consideration we can specify the shift along each G_μ-orbit associated with each iteration of the map.

The papers of Simo and Wong [1989] and Krishnaprasad and Austin [1990] provide examples of how to make the choices required in steps (1), (2), and (3).

Appendix C: The Hopf Fibration in Mechanics

The Hopf fibration is a mapping from S^3 to S^2. Using the fact that S^3 is topologically equivalent to the set of unit quaternions, which is in turn isomorphic to $SU(2)$, the following diagram for the Hopf fibration is obtained:

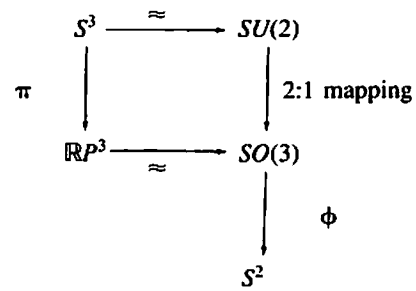

where π is a quotient map which identifies antipodal points of S^3 and ϕ is the map taking $A \in SO(3) \to Ak \in S^2$. Here k is a fixed

unit vector in $\mathbb{R}^3$. The composition $\phi \circ \pi$ is the Hopf map, but by an abuse of notation we also call ϕ the Hopf map.

The Hopf fibration has two realizations that are pertinent to mechanics: the reduction procedure for the rigid body and for the 1 : 1 resonance of two harmonic oscillators. For the rigid body, $\mathfrak{so}(3)^*$ is interpreted as the body angular momentum space of a rigid body and the momentum map is a map $J : T^*SO(3) \to \mathfrak{so}(3)^*$. A level set of J is $J^{-1}(\mu) \subset T^*SO(3)$ for $\mu \in \mathfrak{so}(3)^*$. We may identify $J^{-1}(\mu)$ with $SO(3)$ by means of the one-to-one map $\psi(A) = R_A\mu$, where $A \in SO(3)$ and R_A is right translation by A. Recalling that G_μ denotes the group of rotations about the axis determined by μ, we realize the map ϕ as

$$\begin{array}{ccc} & \text{Hopf map } \phi & \\ SO(3) & \longrightarrow & S^2 \\ \psi \downarrow & & \downarrow \approx \\ J^{-1}(\mu) & \longrightarrow & J^{-1}(\mu)/G_\mu \\ & \text{quotient} & \end{array}$$

The quotient projection can be interpreted as a momentum map corresponding to the right action of $SO(3)$ on itself.

In the second application to mechanics, the Hopf fibration is applied to a Hamiltonian system of two harmonic oscillators which are in a 1 : 1 resonance. The Hamiltonian for this system is given by

$$H = \frac{1}{2}(p_1^2 + q_1^2 + p_2^2 + q_2^2),$$

and the orbits of this system lie on the level sets $H = h$ in $\mathbb{C}^2$ which are three-spheres of radius $\sqrt{2h}$. As in Koçak et al. [1986], we define Hopf variables w_1, w_2, w_3, w_4 by

$$\begin{aligned} w_1 &= 2(q_1q_2 + p_1p_2), \\ w_2 &= 2(q_1p_2 - q_2p_1), \\ w_3 &= (q_1^2 + p_1^2) - (q_2^2 + p_2^2), \\ w_4 &= 2h. \end{aligned}$$

These variables satisfy $w_1^2 + w_2^2 + w_3^2 = w_4^2$ and so the Hopf fibration maps

$$S^3 \cong (q_1,p_1,q_2,p_2) \to (w_1,w_2,w_3) \cong S^2.$$

In complex notation, the Hopf fibration is even easier to describe. We write $z_1 = q_1 + p_1$ and $z_2 = q_2 + p_2$ so that the Hamiltonian becomes

$$H = \frac{1}{2}(|z_1|^2 + |z_2|^2),$$

which is symmetric under $SU(2)$. The momentum map of $SU(2)$ acting on $\mathbb{C}^2$ is exactly

$$(q_1,p_1,q_2,p_2) \to (w_1,w_2,w_3),$$

and its restriction to μ = constant maps S^3 to S^2 as above, *i.e., the Hopf fibration is a momentum map*. In fact, these two examples are related: Cushman and Rod [1982] have shown how to analyze the 1:1 resonance using grid body dynamics!

References

R. Abraham and J. Marsden [1978] *Foundations of Mechanics*. 2nd edition, Addison Wesley, Reading, MA, 1985.

D. Armbruster, J. Guckenheimer, and S. Kim [1989] Chaotic dynamics in systems with square symmetry, *Phys. Lett. A*, **40**, 416–420.

V. Arnold [1978] *Mathematical Methods of Classical Mechanics*, 2nd ed., K. Vogtmann and A. Weinstein, trans., Springer-Verlag, New York.

J. Baillieul and M. Levi [1987] Rotational elastic dynamics, *Physica D*, **27**, 43–62.

M. Berry [1988] The geometric phase, *Scientific American*, December.

R. W. Brockett [1987] On the control of vibratory actuators, *Proc. 1987 IEEE Conf. Decision and Control*, 1418–1422.

R. W. Brockett [1989] On the rectification of vibratory motion, *Sensors and Actuators*, **20**, 91–96.

P. Channell [1983] Symplectic integration algorithms, Los Alamos National Laboratory Report AT-6: ATN-83-9.

P. Channell and C. Scovel [1990] Symplectic integration of Hamiltonian systems, *Nonlinearity*, **3**, 231–259.

R. Cherry [1989] Letter to the editor, *Scientific American*, March 9.

A. Chorin, T. J. R. Hughes, J. E. Marsden and M. McCracken [1978] *Commun. Pure Appl. Math.*, **31**, 205.

R. Cushman, D. Rod [1982] Reduction of the semi-simple 1:1 resonance, *Physica D*, **6**, 105–112.

R. DeVogelaére [1956] Methods of integration which preserve the contact transformation property of the Hamiltonian equations, Department of Mathematics, University of Notre Dame Report **4**.

Ge Zhong [1988] Geometry in symplectic difference schemes and generating functions. Preprint.

Ge Zhong and J. Marsden [1988] Lie-Poisson Hamilton-Jacobi theory and Lie-Poisson integrators, *Phys. Lett A*, **133**, 134–139.

H. Goldstein [1980] *Classical Mechanics*. 2nd edition, Addison-Wesley, Reading, MA.

D. Greenspan [1974] *Discrete Numerical Methods in Physics and Engineering*. Academic Press, New York.

D. Greenspan [1984] Conservative methods for $\ddot{x} = f(x)$, *J. Comput. Phys.*, **56**, 28–41.

Y. Ise [1986] Traveling wave ultrasonic motors offer high concession efficiency, *J. Elect. Eng.*, 66–70.

H. Koçak, F. Bisshopp, T. Banchoff, and D. Laidlaw [1986] Topology and mechanics, *Adv. Appl. Math.*, **7**, 282–308.

P. S. Krishnaprasad and M. Austin [1990] Symplectic and almost Poisson integration. Preprint.

A. M. Liapunov [1909] Problème génèral de la stabilité du mouvement, reprinted 1949 in *Annals of Mathematical Studies, Vol 17*. Princeton University Press, Princeton.

J. Marsden, R. Montgomery and T. Ratiu [1990] Reduction, symmetry, and phases in mechanics, *Memoirs of the AMS*, **436**.

R. Montgomery, M. Raibert, and Zexing Li [1990] Dynamics and optimal control of legged locomotion systems. Preprint.

A. Shapere [1989] Gauge mechanics of deformable bodies, PhD thesis, Princeton.

A. Shapere and F. Wilczek [1987] Self-propulsion at low Reynolds number, *Phys. Rev. Lett.*, **58**, 2051–2054.

J. C. Simo [1990] Private communication.

J. C. Simo and L. Vu-Quoc [1987] The role of nonlinear theories in transient dynamics analysis of flexible structures, *J. Sound and Vibration*, **119**, 487–508.

J. C. Simo and K. K. Wong [1989] Unconditionally stable algorithms for the orthogonal group that exactly preserve energy and momentum, *Int. J. Num. Meth. Engng.*, **31**, 19–52.

D. Stofer [1987] Some geometric and numerical methods for perturbed integrable systems, Thesis, Zurich.

W. P. Thurston and J. R. Weeks [1986] The mathematics of three-dimensional manifolds, *Scientific American*, **251**, 108–120.

S. Wiggins [1988] *Global Bifurcations and Chaos*, Applied Mathematical Sciences, Vol. 73, Springer-Verlag, New York.

F. Wilczek [1988] Gauge structure of deformable bodies, Princeton preprint, IASSNS -HEP- 88/41.

R. Yang and P. S. Krishnaprasad [1990] On the dynamics of floating four-bar linkages, *IEEE Conference on Decision and Control* 1288–1293.

Xie Zhi-Yun [1990] Conservative numerical schemes for Hamiltonian systems, *J. Comput. Phys.* (to appear).